

Product Wave Function Renormalization Group: construction from the matrix product point of view

Kouji UEDA, Tomotoshi NISHINO, Kouichi OKUNISHI,²⁾ Yasuhiro HIEIDA,³⁾
Rene DERIAN,⁴⁾ and Andrej GENDIAR⁴⁾

Department of Physics, Faculty of Science, Kobe University, Kobe 657-8501

²⁾ *Department of Physics, Faculty of Science, Niigata University, Igarashi 2, Niigata 950-2181*

³⁾ *Computer and Network Center, Saga University, Saga 840-8502*

⁴⁾ *Institute of Electrical Engineering, Slovak Academy of Sciences, Dúbravská cesta 9, SK-841 04 Bratislava, Slovakia*

(Received)

We present a construction of a matrix product state (MPS) that approximates the largest-eigenvalue eigenvector of a transfer matrix T , for the purpose of rapidly performing the infinite system density matrix renormalization group (DMRG) method applied to two-dimensional classical lattice models. We use the fact that the largest-eigenvalue eigenvector of T can be approximated by a state vector created from the upper or lower half of a finite size cluster. Decomposition of the obtained state vector into the MPS gives a way of extending the MPS, at the system size increment process in the infinite system DMRG algorithm. As a result, we successfully give the physical interpretation of the product wave function renormalization group (PWFRG) method, and obtain its appropriate initial condition.

§1. Introduction

Calculation of the maximum eigenvalue of a transfer matrix is one of the most fundamental task in statistical mechanics of lattice models. In two dimensional (2D) classical systems, the density matrix renormalization group (DMRG) method is a powerful tool for this purpose,¹⁻⁴⁾ where the maximum eigenvalue is variationally evaluated by implicit use of the matrix product state (MPS).⁵⁻¹²⁾

In actual applications of the DMRG method to classical models, most of the computational time is consumed for the determination of the largest-eigenvalue eigenvector of the renormalized transfer matrix.^{2,3)} The matrix product structure of the variational state helpfully tells us how to save the computational time. For instance, in the *finite* system DMRG algorithm,⁴⁾ a good trial vector for the diagonalization of the renormalized transfer matrix can be constructed from the MPS.^{13,14)} For the *infinite* system DMRG algorithm, however, such preparation of the trial vector is rather difficult, since we have to extrapolate the MPS — increase the number of matrices — toward a larger system size.

The solution of this problem is partially achieved by the product wave function renormalization group (PWFRG) method, which increases the number of matrices in the MPS on the basis of the relation between block-spin transformations.¹⁵⁾ The numerical efficiency of the PWFRG method has been demonstrated for classical systems^{16,17)} as well as quantum ones.¹⁸⁻²²⁾ In spite of the efficiency of the PWFRG method, we have two problems to be solved from theoretical view point. One is in the physical interpretation of the extrapolation of the MPS, in particular, when the system size is small. This is because the extension process has been justified only in

the thermodynamic limit. Another is in the preparation of initial matrices, which is necessary to start the recursive computation of the PWFRG method. So far these matrices are set empirically, which may not guarantee the numerical stability.

To find the solution of the above problems of the PWFRG method, it is instructive to recall the physical substance of the Baxter's corner transfer matrix (CTM) method²³⁾ or its variant, the corner transfer matrix renormalization group (CTMRG) method.^{24,25)} These CTM type methods calculate the partition function of the finite size cluster recursively, where the number of iterations corresponds to the linear dimension of the system. A preferable point on the methods is that the initial condition is well-defined as CTMs with appropriate boundary spin configurations. In this paper, we import such well-controllable aspects of the CTM-type methods into the extension process of the MPS.

In the next section we consider a way of the extension of the finite size clusters, which can be regarded as a variant of the CTMRG method. In §3 we analyze the MPS structure of the approximate largest-eigenvalue eigenvectors generated by the recursive extension process obtained in §2. We successfully give the physical interpretation of the PWFRG method, and reconstruct its numerical algorithm, which includes the appropriate initial condition. In the last section, we conclude the obtained results.

§2. Recursive Construction of State Vectors

As an example of 2D statistical models, let us consider the interaction-round-a-face (IRF) model, which contains the Ising model as its special case. The IRF model is defined by the local Boltzmann Weight $W(s'\sigma'|s\sigma)$ assigned for each face of the square lattice, where $s,$

s' , σ and σ' represent q -state spin variables on lattice points. (See Fig.1.) For simplicity, we consider 2-state Ising spins ($q = 2$) and assume the symmetry $W(s'\sigma'|s\sigma) = W(\sigma'\sigma'|s\sigma)$ and $W(s'\sigma'|s\sigma) = W(s\sigma|s'\sigma')$ throughout this article.²⁶⁾ Let us consider the finite size cluster of width $2N$ shown in Fig.1.²⁷⁾ The partition function of the cluster is given by the spin configuration sum of the product of all the Boltzmann weights in the cluster

$$Z_N = \sum \prod W, \quad (2.1)$$

where we have omitted spin variables for simplicity. Throughout this section we assume the free boundary condition.

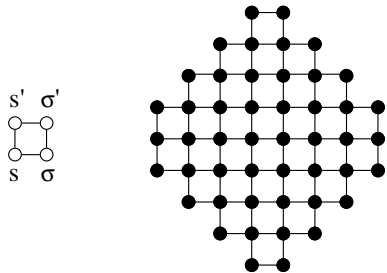


Fig. 1. The arrangement of spins of the local Boltzmann weight $W(s'\sigma'|s\sigma)$ (in the left) and the finite size cluster of width $2N$ considered in the partition function Z_N in Eq.(2.1) (in the right). We show the case $N = 4$, equivalently, $2N = 8$.

We divide the system into the upper and lower halves. Figure 2(a) shows the lower half of the system, where we label the spins on the cut as $s_1 \dots s_N \sigma_N \dots \sigma_1$ from the left to right. Considering the product of local Boltzmann weights in the lower half, and taking the configuration sum of spins except for $s_1 \dots s_N \sigma_N \dots \sigma_1$, we obtain a 2^{2N} -dimensional vector $|\Psi_N\rangle$ whose elements are $\Psi_N[s_1 \dots s_N \sigma_N \dots \sigma_1]$. In the same manner we obtain the 2^{2N} -dimensional vector $\langle\Psi_N|$ that corresponds to the upper half of the original cluster. Let us call these vectors *state vectors* in the following. By definitions of $\langle\Psi_N|$ and $|\Psi_N\rangle$, the partition function in Eq.(2.1) is expressed by the inner product

$$Z_N = \langle\Psi_N|\Psi_N\rangle. \quad (2.2)$$

Let us introduce the row-to-row transfer matrix

$$\begin{aligned} T_N[s'_1 \dots s'_N \sigma'_N \dots \sigma'_1 | s_1 \dots s_N \sigma_N \dots \sigma_1] \\ = W(s'_1 s'_2 | s_1 s_2) W(s'_2 s'_3 | s_2 s_3) \cdots W(\sigma'_2 \sigma'_1 | \sigma_2 \sigma_1). \end{aligned} \quad (2.3)$$

For simplicity, we introduce ‘dot product notation’ with which we abbreviate eq.(2.3) as $T_N = W \cdot W \cdots W$.

The state vector $|\Psi_N\rangle$ can be used as a good variational vector for T_N , when the system is off critical and N is sufficiently larger than the correlation length.²³⁾ This is because the variational ratio

$$g = \frac{\langle\Psi_N|T_N|\Psi_N\rangle}{\langle\Psi_N|\Psi_N\rangle} = \frac{\langle\Psi_N|T_N|\Psi_N\rangle}{Z_N} \quad (2.4)$$

well approximates the largest-eigenvalue of T_N in the sense that, as N increases, $f = -(k \ln g) / 2N$ where k is the Boltzmann constant approaches to the free energy

per site in the thermodynamic limit.

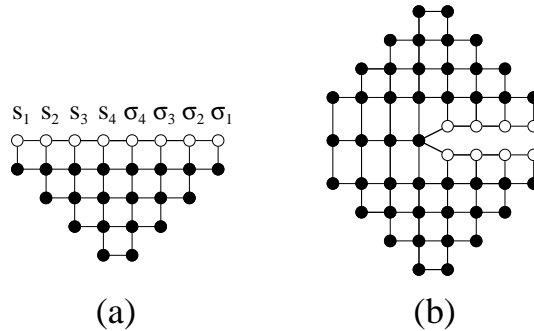


Fig. 2. Graphical representations: (a) The state vector $|\Psi_N\rangle$ when $N = 4$. (b) The reduced density matrix ρ_N^R . Black dots denote spin variables that are summed.

We occasionally interpret $|\Psi_N\rangle$ as a $2^N \times 2^N$ matrix Ψ_N , whose elements $\Psi_N(s_N \dots s_1 | \sigma_N \dots \sigma_1)$ are equal to $\Psi_N[s_1 \dots s_N \sigma_N \dots \sigma_1]$. (We have put the vertical line $|$ between the first matrix index $s_N \dots s_1$ and the second one $\sigma_N \dots \sigma_1$, respectively, which corresponds to the left and the right half-row spins. We reverse the spin order as $s_N \dots s_1$ for the later convenience.) This notation is useful when we consider the reduced density matrix $\rho_N^R = \text{Tr}_L |\Psi_N\rangle \langle\Psi_N|$, where Tr_L represents the spin contraction for all the s_i in the left side. Figure 2(b) shows the graphical representation of ρ_N^R .^{2, 23, 24)} Using the matrix notation Ψ_N we can simply write ρ_N^R as the matrix product $\Psi_N^\dagger \Psi_N$, since the elements of ρ_N^R are explicitly given by

$$\begin{aligned} \rho_N^R(\sigma'_N \dots \sigma'_1 | \sigma_N \dots \sigma_1) = \sum_{s_N \dots s_1} \Psi_N(s_N \dots s_1 | \sigma'_N \dots \sigma'_1) \\ \Psi_N(s_N \dots s_1 | \sigma_N \dots \sigma_1). \end{aligned} \quad (2.5)$$

Similarly we obtain the reduced density matrix for the left side $\rho_N^L = \text{Tr}_R |\Psi_N\rangle \langle\Psi_N| = \Psi_N \Psi_N^\dagger$. It should be noted that all the elements of Ψ_N , ρ_N^R and ρ_N^L are real and non negative. The partition function in Eq.(2.2) is expressed as

$$Z_N = \text{Tr} \rho_N^L = \text{Tr} \rho_N^R = \text{Tr} \Psi_N^\dagger \Psi_N. \quad (2.6)$$

In the following we consider a recursive construction of Ψ_N , starting from $N = 1$ up to a certain system size. Let us first take the configuration sum for 2 spins on the local Boltzmann weight

$$\Psi_1(s'_1 | \sigma'_1) = \sum_{s_1 \sigma_1} W(s'_1 \sigma'_1 | s_1 \sigma_1) \quad (2.7)$$

to obtain a state vector $|\Psi_1\rangle$ of the smallest width. (See Fig.2(a) and imagine the case $N = 1$.) In order to extend the system size and construct $|\Psi_2\rangle$, consider the row-to-row transfer matrix $T_2 \equiv W \cdot W \cdot W$, whose elements are expressed as

$$\begin{aligned} T_2[s'_1 s'_2 \sigma'_2 \sigma'_1 | s_1 s_2 \sigma_2 \sigma_1] \\ = W(s'_1 s'_2 | s_1 s_2) W(s'_2 \sigma'_2 | s_2 \sigma_2) W(\sigma'_2 \sigma'_1 | \sigma_2 \sigma_1). \end{aligned} \quad (2.8)$$

(See Fig.3(a).) It is convenient to define half-row transfer matrices for both the left and the right parts of the transfer matrix. For Eq.(2.8), we have

$$\begin{aligned} T_2^R(\sigma'_2\sigma'_1|\sigma_2\sigma_1) &= W(\sigma'_2\sigma'_1|\sigma_2\sigma_1) \\ T_2^L(s'_2s'_1|s_2s_1) &= W(s'_1s'_2|s_1s_2), \end{aligned} \quad (2.9)$$

where the order of spin indices in T_2^L is reversed for convenience, so that $T_2^L = T_2^R$ holds when W is symmetric. To obtain $|\Psi_2\rangle$, we “join” $T_2 \equiv T_2^L \cdot W \cdot T_2^R$ to $|\Psi_1\rangle$ as follows. First we contract a spin in the half-row transfer matrices as

$$\begin{aligned} P_2^R(\sigma'_2\sigma'_1|\sigma_2) &= \sum_{\sigma_1} T_2^R(\sigma'_2\sigma'_1|\sigma_2\sigma_1) \\ P_2^L(s'_2s'_1|s_2) &= \sum_{s_1} T_2^L(s'_2s'_1|s_2s_1). \end{aligned} \quad (2.10)$$

For the later use we define a $2^4 \times 2^2$ matrix $P_2 \equiv P_2^L \cdot W \cdot P_2^R$ shown in Fig.3(b), whose elements are given by

$$\begin{aligned} P_2[s'_1s'_2\sigma'_2\sigma'_1|s_2\sigma_2] \\ = P_2^L(s'_2s'_1|s_2)W(s'_2\sigma'_2|s_2\sigma_2)P_2^R(\sigma'_2\sigma'_1|\sigma_2). \end{aligned} \quad (2.11)$$

Then we can obtain $|\Psi_2\rangle$ by applying P_2 to $|\Psi_1\rangle$ as shown in Fig.3(c), where the matrix elements of Ψ_2 is explicitly given by

$$\begin{aligned} \Psi_2(s'_2s'_1|\sigma'_2\sigma'_1) &= \sum_{s_2\sigma_2} P_2^L(s'_2s'_1|s_2) \\ &\times W(s'_2\sigma'_2|s_2\sigma_2)P_2^R(\sigma'_2\sigma'_1|\sigma_2)\Psi_1(s_2|\sigma_2). \end{aligned} \quad (2.12)$$

It should be noted that the variables contained in Ψ_1 are s_2 and σ_2 only. In short, we write Eq.(2.12) as $|\Psi_2\rangle = P_2^L \cdot W \cdot P_2^R |\Psi_1\rangle$.

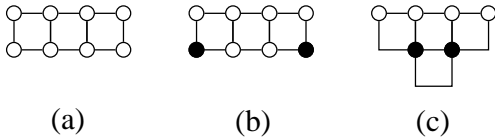


Fig. 3. Graphical representations: (a) Transfer matrix $T_2 \equiv W \cdot W \cdot W = T_2^L \cdot W \cdot T_2^R$ in Eq.(2.8). (b) $P_2 \equiv P_2^L \cdot W \cdot P_2^R$ in Eq.(2.11). (c) The extension process of the state vector $P_2^L \cdot W \cdot P_2^R |\Psi_1\rangle$ in Eq.(2.12).

In the same manner we obtain $|\Psi_3\rangle$ by applying $P_3 \equiv P_3^L \cdot W \cdot P_3^R$ to $|\Psi_2\rangle$, where the matrix elements of $P_3^R \equiv W \cdot P_2^R$ are given by

$$P_3^R(\sigma'_3\sigma'_2\sigma'_1|\sigma_3\sigma_2) = W(\sigma'_3\sigma'_2|\sigma_3\sigma_2)P_2^R(\sigma'_2\sigma'_1|\sigma_2). \quad (2.13)$$

Hereafter we do not refer to the calculations of T_N^L , P_N^L , and ρ_N^L for book keeping purpose.

Since such recursive extensions of $|\Psi_N\rangle$ cause the exponential blow-up of the vector (or matrix) dimensions, we have to introduce the density matrix renormalization to reduce the dimensions below a certain number m .^{1,2)} The value of m is normally chosen to be $10 \sim 1000$. (In the following explanation we assume $m \geq 8$.) Let us consider the case $N = 2$ as an example. We diagonalize

the reduced density matrix

$$\begin{aligned} \rho_2^R(\sigma'_2\sigma'_1|\sigma_2\sigma_1) &= \sum_{s_2s_1} \Psi_2(s_2s_1|\sigma'_2\sigma'_1)\Psi_2(s_2s_1|\sigma_2\sigma_1) \\ &= \sum_{\xi_2} U_2(\sigma'_2\sigma'_1|\xi_2)\lambda_2(\xi_2)U_2(\sigma_2\sigma_1|\xi_2), \end{aligned} \quad (2.14)$$

where we assume the decreasing order for the eigenvalues $\lambda_2(\xi_2)$, which are non-negative. As in the DMRG method, the matrix U_2 plays a role of the block spin transformation from the group of 2 spins $\sigma_2\sigma_1$ to a new block spin variable ξ_2 , which takes 4 states. By operating U_2^\dagger to P_3^R , we obtain the renormalized matrix \tilde{P}_3^R as

$$\tilde{P}_3^R(\sigma'_3\xi_2|\sigma_3\sigma_2) = \sum_{\sigma'_2\sigma'_1} U_2(\sigma'_2\sigma'_1|\xi_2)P_3^R(\sigma'_3\sigma'_2\sigma'_1|\sigma_3\sigma_2) \quad (2.15)$$

which is graphically represented in Fig.4. Here we should remark that, in strict sense, the r.h.s. of Eq.(2.15) is not a simple matrix multiplication between U_2^\dagger and P_3^R , since U_2^\dagger works only on σ'_2 and σ'_1 . Keeping this point in mind, we compactly write Eq.(2.15) as $\tilde{P}_3^R = \hat{U}_2^\dagger P_3^R$. In the following, we shall put “hat” symbol on matrices that play a role of the block spin transformations and “tilde” on vectors and matrices generated by the block spin transformations. Applying $\tilde{P}_3 \equiv \tilde{P}_3^L \cdot W \cdot \tilde{P}_3^R$ to $|\Psi_2\rangle$ we obtain an extended state vector

$$\begin{aligned} \tilde{\Psi}_3(s'_3\zeta_2|\sigma'_3\xi_2) &= \sum_{s_3s_2\sigma_3\sigma_2} \tilde{P}_3^L(s'_3\zeta_2|s_3s_2) \\ &\times W(s'_3\sigma'_3|s_3\sigma_3)\tilde{P}_3^R(\sigma'_3\xi_2|\sigma_3\sigma_2)\Psi_2(s_3s_2|\sigma_3\sigma_2), \end{aligned} \quad (2.16)$$

which contains block spin variables as shown in Fig.5(a). Since the block-spin transformation is exact, the relation $Z_3 = \langle \Psi_3 | \Psi_3 \rangle = \langle \tilde{\Psi}_3 | \tilde{\Psi}_3 \rangle$ is satisfied.

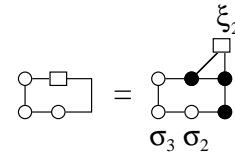


Fig. 4. The block spin transformation $\tilde{P}_3^R = \hat{U}_2^\dagger P_3^R$ in Eq.(2.15).

Let us continue the system extension process. We diagonalize the reduced density matrix

$$\begin{aligned} \tilde{\rho}_3^R(\sigma'_3\xi'_2|\sigma_3\xi_2) &= \sum_{s_3\zeta_2} \tilde{\Psi}_3(s_3\zeta_2|\sigma'_3\xi'_2)\tilde{\Psi}_3(s_3\zeta_2|\sigma_3\xi_2) \\ &= \sum_{\xi_3} U_3(\sigma'_3\xi'_2|\xi_3)\lambda_3(\xi_3)U_3(\sigma_3\xi_2|\xi_3) \end{aligned} \quad (2.17)$$

in order to obtain the block spin transformation \hat{U}_3 that maps $\sigma_3\xi_2$ to the 8-state block spin ξ_3 . This time we perform the extension from \tilde{P}_3^R to \tilde{P}_4^R operating \hat{U}_3^\dagger from

the left and \hat{U}_2 from the right

$$\begin{aligned} \tilde{P}_4^R(\sigma'_4 \xi_3 | \sigma_4 \eta_3) &= \sum_{\sigma'_3 \xi_2 \sigma_3 \sigma_2} U_3(\sigma'_3 \xi_2 | \xi_3) W(\sigma'_4 \sigma'_3 | \sigma_4 \sigma_3) \\ &\times \tilde{P}_3^R(\sigma'_3 \xi_2 | \sigma_3 \sigma_2) U_2(\sigma_3 \sigma_2 | \eta_3) \end{aligned} \quad (2.18)$$

as shown in Fig.5(b), or in short $\tilde{P}_4^R \equiv \hat{U}_3^\dagger(W \cdot \tilde{P}_3^R)\hat{U}_2$. (Note that the matrix U_2 in the right hand side contains σ_3 and σ_2 , not σ_2 and σ_1 .) Up to this stage, we keep all the block spin states since we have assumed $m \geq 8$.

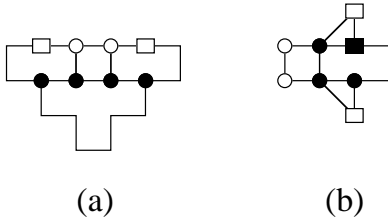


Fig. 5. Graphical representations: (a) Extension from $|\Psi_2\rangle$ to $|\Psi_3\rangle = \tilde{P}_3^R|\Psi_2\rangle$ in Eq.(2.16). (b) Extension from \tilde{P}_3^R to $\tilde{P}_4^R \equiv \hat{U}_3^\dagger(W \cdot \tilde{P}_3^R)\hat{U}_2$ in Eq.(2.18).

Now we can generalize the extension process up to arbitrary system size. If we have $|\tilde{\Psi}_i\rangle$ up to a certain size $i \geq 2$, we can construct the extended one

$$|\tilde{\Psi}_{i+1}\rangle = \tilde{P}_{i+1}|\tilde{\Psi}_i\rangle = \tilde{P}_{i+1}^L \cdot W \cdot \tilde{P}_{i+1}^R |\tilde{\Psi}_i\rangle \quad (2.19)$$

with

$$\tilde{P}_{i+1}^R \equiv \hat{U}_i^\dagger(W \cdot \tilde{P}_i^R)\hat{U}_{i-1}, \quad (2.20)$$

where the block spin transformations \hat{U}_i and \hat{U}_{i-1} have been obtained by the diagonalizations of $\tilde{\rho}_i^R$ and $\tilde{\rho}_{i-1}^R$, respectively. The matrix elements of Eq.(2.19) and (2.20) are explicitly given by

$$\begin{aligned} \tilde{\Psi}_{i+1}(s'_{i+1} \zeta_i | \sigma'_{i+1} \xi_i) &= \\ \sum_{s_{i+1} \mu_i \sigma_{i+1} \eta_i} \tilde{P}_{i+1}^L(s'_{i+1} \zeta_i | s_{i+1} \mu_i) W(s'_{i+1} \sigma'_{i+1} | s_{i+1} \sigma_{i+1}) \\ &\times \tilde{P}_{i+1}^R(\sigma'_{i+1} \xi_i | \sigma_{i+1} \eta_i) \tilde{\Psi}_i(s_{i+1} \mu_i | \sigma_{i+1} \eta_i) \end{aligned} \quad (2.21)$$

and

$$\begin{aligned} \tilde{P}_{i+1}^R(\sigma'_{i+1} \xi_i | \sigma_{i+1} \eta_i) &= \sum_{\sigma'_i \xi_{i-1} \sigma_i \eta_{i-1}} U_i(\sigma'_i \xi_{i-1} | \xi_i) \\ &\times W(\sigma'_{i+1} \sigma'_i | \sigma_{i+1} \sigma_i) \tilde{P}_i^R(\sigma'_i \xi_{i-1} | \sigma_i \eta_{i-1}) U_{i-1}(\sigma_i \eta_{i-1} | \eta_i). \end{aligned} \quad (2.22)$$

The key point in Eqs.(2.20) and (2.22) is that the label of U_i is larger than that of U_{i-1} by one, which enables us to "extrapolate" the state vector in Eqs.(2.19) and (2.21).

As is performed in the DMRG method, we keep at most m numbers of relevant states for the block spin variables, and neglect the rest of irrelevant ones in Eq.(2.20). We can thus calculate the approximate partition func-

tion $\tilde{Z}_i = \langle \tilde{\Psi}_i | \tilde{\Psi}_i \rangle$ recursively up to arbitrary system size $i = N$. In addition to \tilde{Z}_N , we can obtain the nearest neighbor spin correlation function

$$\langle s_N \sigma_N \rangle = \frac{\langle \tilde{\Psi}_N | s_N \sigma_N | \tilde{\Psi}_N \rangle}{\langle \tilde{\Psi}_N | \tilde{\Psi}_N \rangle} \quad (2.23)$$

at the center of the system.

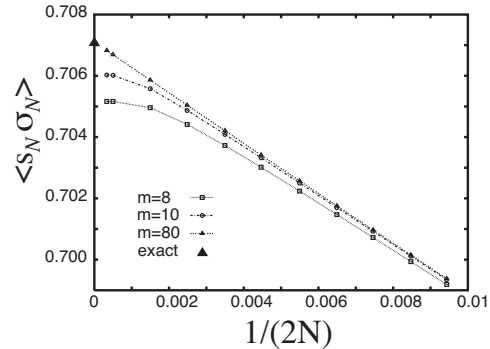


Fig. 6. Nearest neighbor spin correlation function $\langle s_N \sigma_N \rangle$ in Eq.(2.23) of the Ising model at criticality.

Let us observe the numerical efficiency of the explained recursive algorithm in the application to the Ising model. Figure 6 shows the calculated $\langle s_N \sigma_N \rangle$ at criticality where the correlation length is infinite. The calculated data deviates from the scaling line when the system size exceeds the artificial cut-off length introduced by the restriction of the degrees of freedom down to m . The observed cut-off effect is similar to that of the CTMRG method.^{24,25} This is because the system-size extension process defined by Eq.(2.19) and (2.20) is quite similar to the extension of the corner transfer matrix in the CTMRG method.

§3. Product Wave Function Renormalization Group

It is worth looking at the structure of $\tilde{P}_i \equiv \tilde{P}_i^L \cdot W \cdot \tilde{P}_i^R$ from the view point of the MPS.⁶⁻⁸ Tracing back the recursive construction in Eqs.(2.10), (2.15), (2.18), and (2.20), we can represent $\tilde{P}_i^R(\sigma'_i \xi_{i-1} | \sigma_i \eta_{i-1})$ for $i \geq 6$ as

$$\begin{aligned} \tilde{P}_i^R &\equiv \hat{U}_{i-1}^\dagger(W \cdot \tilde{P}_{i-1}^R)\hat{U}_{i-2} \\ &= \hat{U}_{i-1}^\dagger(W \cdot \hat{U}_{i-2}^\dagger(W \cdot \tilde{P}_{i-2}^R)\hat{U}_{i-3})\hat{U}_{i-2} \\ &= \hat{U}_{i-1}^\dagger(W \cdot \hat{U}_{i-2}^\dagger(W \cdot (\dots(W \cdot P_2^R)\dots)\hat{U}_{i-3})\hat{U}_{i-2}. \end{aligned} \quad (3.1)$$

Introducing the 2^i by 2^{i-1} matrix $P_i^R(\sigma'_i \dots \sigma'_1 | \sigma_i \dots \sigma_2)$, which is defined by $P_i^R \equiv W \cdot P_{i-1}^R = (W \cdot)^{i-2} P_2^R$, we rewrite Eq.(3.1) as the simpler form

$$\tilde{P}_i^R \equiv \hat{U}_{i-1}^\dagger \dots \hat{U}_3^\dagger \hat{U}_2^\dagger P_i^R \hat{U}_2 \hat{U}_3 \dots \hat{U}_{i-2}, \quad (3.2)$$

where $\hat{U}_{i-1}^\dagger \dots \hat{U}_3^\dagger \hat{U}_2^\dagger$ represents the successive block spin transformations by $U_2(\sigma'_2 \sigma'_1 | \xi_2)$, $U_3(\sigma'_3 \xi_2 | \xi_3) \dots$, and $U_{i-1}(\sigma'_{i-1} \xi_{i-2} | \xi_{i-1})$. In the same manner $\hat{U}_2 \hat{U}_3 \dots \hat{U}_{i-2}$ represents the successive block spin transformations by $U_2(\sigma_3 \sigma_2 | \eta_3)$, $U_3(\sigma_4 \eta_3 | \eta_4) \dots$, and $U_{i-2}(\sigma_{i-1} \eta_{i-2} | \eta_{i-1})$, where one should pay attention to the indices of spin variables. The structure of \tilde{P}_i^R is similar to that of the

renormalized half-row transfer matrix

$$\begin{aligned}
\tilde{T}_i^{\text{R}} &\equiv \hat{U}_{i-1}^\dagger (W \cdot \tilde{T}_{i-1}^{\text{R}}) \hat{U}_{i-1} \\
&= \hat{U}_{i-1}^\dagger (W \cdot \hat{U}_{i-2}^\dagger (W \cdot (\dots (W \cdot T_2^{\text{R}}) \dots) \hat{U}_{i-2}) \hat{U}_{i-1} \\
&= \hat{U}_{i-1}^\dagger \dots \hat{U}_3^\dagger \hat{U}_2^\dagger (W \dots W \cdot T_2^{\text{R}}) \hat{U}_2 \hat{U}_3 \dots \hat{U}_{i-1} \\
&= \hat{U}_{i-1}^\dagger \dots \hat{U}_3^\dagger \hat{U}_2^\dagger T_i^{\text{R}} \hat{U}_2 \hat{U}_3 \dots \hat{U}_{i-1}, \quad (3.3)
\end{aligned}$$

which has been used in the DMRG method. (We have introduced $T_i^{\text{R}} = W \cdot T_{i-1}^{\text{R}} = (W \cdot)^{i-2} T_2^{\text{R}}.$) In Eq.(3.3) the successive block spin transformations $\hat{U}_{i-1}^\dagger \dots \hat{U}_3^\dagger \hat{U}_2^\dagger$ are the conjugate of $\hat{U}_{i-1} \dots \hat{U}_3 \hat{U}_2$, and are performed by the matrices $U_2(\sigma_2 \sigma_1 | \xi_2)$, $U_3(\sigma_3 \xi_2 | \xi_3) \dots$, and $U_{i-1}(\sigma_{i-1} \xi_{i-2} | \xi_{i-1})$. Comparing Equations (3.2) and (3.3), let us consider the relation between the renormalization process explained in the previous section and that in the conventional DMRG method.

Since the structure of \tilde{T}_i^{R} in Eq.(3.3) is similar to that of \tilde{P}_i^{R} in Eq.(3.2), we try to handle \tilde{P}_i^{R} and \tilde{T}_i^{R} in a unified manner. Let us introduce a new matrix V_1 , whose elements are given by

$$V_1(\sigma_2 \sigma_1 | \sigma_2') = \delta(\sigma_2 | \sigma_2'), \quad (3.4)$$

which is independent of σ_1 , and the right hand side is the Kronecker delta. The matrix V_1 has a function of taking configuration sum for σ_1 as Eq.(2.10), when it is operated to the half-row transfer matrices. For example, we obtain

$$\begin{aligned}
&P_i^{\text{R}}(\sigma_i' \dots \sigma_1' | \sigma_i \dots \sigma_2) \\
&= \sum_{\sigma_2'' \sigma_1''} T_i^{\text{R}}(\sigma_i' \dots \sigma_1' | \sigma_i \dots \sigma_3 \sigma_2'' \sigma_1'') V_1(\sigma_2'' \sigma_1'' | \sigma_2) \\
&= \sum_{\sigma_1} T_i^{\text{R}}(\sigma_i' \dots \sigma_1' | \sigma_i \dots \sigma_2 \sigma_1), \quad (3.5)
\end{aligned}$$

which we compactly write as $P_i^{\text{R}} = T_i^{\text{R}} \hat{V}_1$. Then we can rewrite \tilde{P}_i^{R} in Eq.(3.2) as

$$\tilde{P}_i^{\text{R}} = \hat{U}_{i-1}^\dagger \dots \hat{U}_3^\dagger \hat{U}_2^\dagger T_i^{\text{R}} \hat{V}_1 \hat{U}_2 \hat{U}_3 \dots \hat{U}_{i-2}. \quad (3.6)$$

Note that V_1 in Eq.(3.4) represents the free boundary condition of the system under consideration. For the system with fixed boundary condition $\sigma_1 = 1$, the r.h.s of Eq.(3.4) should be replaced by $\delta(\sigma_2 | \sigma_2') \delta(\sigma_1 | 1)$.

For the moment let us consider the ideal case $m = 2^{i-1}$, where we keep all the states for every block spin transformations. In such a case the block spin transformation is exact, and the relation

$$\begin{aligned}
&\left[\hat{U}_2 \hat{U}_3 \dots \hat{U}_{i-1} \right] \left[\hat{U}_2 \hat{U}_3 \dots \hat{U}_{i-1} \right]^\dagger = \quad (3.7) \\
&\left[\hat{U}_2 \hat{U}_3 \dots \hat{U}_{i-1} \right] \left[\hat{U}_{i-1}^\dagger \dots \hat{U}_3^\dagger \hat{U}_2^\dagger \right] = I_{i-1}
\end{aligned}$$

is satisfied for the transformation matrices $U_2(\sigma_2 \sigma_1 | \xi_2)$, $U_3(\sigma_3 \xi_2 | \xi_3) \dots$, and $U_{i-1}(\sigma_{i-1} \xi_{i-2} | \xi_{i-1})$. The identity I_{i-1} represents $\delta(\sigma_1' | \sigma_1) \delta(\sigma_2' | \sigma_2) \dots \delta(\sigma_{i-1}' | \sigma_{i-1})$, and it satisfies $I_{i-1} = id \cdot I_{i-2} = (id \cdot)^{i-1}$ where id is the local identity $id(\sigma' | \sigma) = \delta(\sigma' | \sigma)$. Putting the identity $I_i = id \cdot I_{i-1}$ after T_i^{R} in Eq.(3.6) and substituting Eq.(3.7),

we obtain

$$\begin{aligned}
\tilde{P}_i^{\text{R}} &= \hat{U}_{i-1}^\dagger \dots \hat{U}_3^\dagger \hat{U}_2^\dagger T_i^{\text{R}} (I_i)^2 \hat{V}_1 \hat{U}_2 \hat{U}_3 \dots \hat{U}_{i-2} \\
&= \left[\hat{U}_{i-1}^\dagger \dots \hat{U}_3^\dagger \hat{U}_2^\dagger T_i^{\text{R}} \hat{U}_2 \hat{U}_3 \dots \hat{U}_{i-1} \right] \\
&\quad \times \left[\hat{U}_{i-1}^\dagger \dots \hat{U}_3^\dagger \hat{U}_2^\dagger I_i \hat{V}_1 \hat{U}_2 \hat{U}_3 \dots \hat{U}_{i-2} \right]. \quad (3.8)
\end{aligned}$$

For convenience, let us define a matrix

$$\begin{aligned}
\tilde{E}_i^{\text{R}} &= \hat{U}_{i-1}^\dagger \dots \hat{U}_3^\dagger \hat{U}_2^\dagger I_i \hat{V}_1 \hat{U}_2 \hat{U}_3 \dots \hat{U}_{i-2} \quad (3.9) \\
&= id \cdot \left(\hat{U}_{i-1}^\dagger \dots \hat{U}_3^\dagger \hat{U}_2^\dagger I_{i-1} \hat{V}_1 \hat{U}_2 \hat{U}_3 \dots \hat{U}_{i-2} \right),
\end{aligned}$$

which satisfies $\tilde{E}_i^{\text{R}} = \hat{U}_{i-1}^\dagger (id \cdot \tilde{E}_{i-1}^{\text{R}}) \hat{U}_{i-2} = id \cdot (\hat{U}_{i-1}^\dagger \tilde{E}_{i-1}^{\text{R}} \hat{U}_{i-2})$, or equivalently

$$\begin{aligned}
\tilde{E}_i^{\text{R}}(\sigma_i' \xi_{i-1} | \sigma_i \eta_{i-1}) &= \delta(\sigma_i' | \sigma_i) \sum_{\sigma_{i-1}' \sigma_{i-1}' \xi_{i-2} \eta_{i-2}} \\
&U_{i-1}(\sigma_{i-1}' \xi_{i-2} | \xi_{i-1}) \tilde{E}_{i-1}^{\text{R}}(\sigma_{i-1}' \xi_{i-2} | \sigma_{i-1}' \eta_{i-2}) \\
&\times U_{i-2}(\sigma_{i-1}' \eta_{i-2} | \eta_{i-1}). \quad (3.10)
\end{aligned}$$

By definition the element $\tilde{E}_i^{\text{R}}(\sigma_i' \xi_{i-1} | \sigma_i \eta_{i-1})$ is zero if $\sigma_i' \neq \sigma_i$. In the same manner we define \tilde{E}_i^{L} , that is the same as \tilde{E}_i^{R} by the assumed symmetry of the system. Substituting Eqs.(3.3) and (3.9) to Eq.(3.8) we obtain the simple relation

$$\tilde{P}_i^{\text{R}} = \tilde{T}_i^{\text{R}} \tilde{E}_i^{\text{R}} \quad (3.11)$$

among the matrices $\tilde{P}_i^{\text{R}}(\sigma_i' \xi_{i-1} | \sigma_i \eta_{i-1})$, $\tilde{T}_i^{\text{R}}(\sigma_i' \xi_{i-1} | \sigma_i' \xi_{i-1}')$, and $\tilde{E}_i^{\text{R}}(\sigma_i' \xi_{i-1}' | \sigma_i \eta_{i-1})$. Introducing the notations $\tilde{E}_i \equiv \tilde{E}_i^{\text{L}} \cdot \tilde{E}_i^{\text{R}}$ and $\tilde{T}_i \equiv \tilde{T}_i^{\text{L}} \cdot W \cdot \tilde{T}_i^{\text{R}}$ we finally reach the relation

$$\tilde{P}_i = \tilde{T}_i \tilde{E}_i \quad (3.12)$$

for the ideal case where there is no cut-off in the block spin transformation.

In realistic numerical calculation we have to neglect irrelevant states, therefore Eqs.(3.7)-(3.12) do not hold exactly, but still \tilde{P}_i is well approximated by $\tilde{T}_i \tilde{E}_i$ if sufficiently large numbers of the block spin states are kept. Under this situation let us consider the operation of \tilde{P}_i to the state vector

$$\begin{aligned}
|\tilde{\Psi}_i\rangle &= \tilde{P}_i |\tilde{\Psi}_{i-1}\rangle \quad (2.19)' \\
&\sim \tilde{T}_i \tilde{E}_i |\tilde{\Psi}_{i-1}\rangle = \tilde{T}_i |\tilde{\Phi}_i\rangle \quad (3.13)
\end{aligned}$$

as shown in Fig.7(a), where the whole structure of \tilde{T}_i is shown in Fig.7(b). We have introduced a new state vector

$$|\tilde{\Phi}_i\rangle = \tilde{E}_i |\tilde{\Psi}_{i-1}\rangle = \tilde{E}_i^{\text{L}} \cdot \tilde{E}_i^{\text{R}} |\tilde{\Psi}_{i-1}\rangle, \quad (3.14)$$

whose structure is shown in Fig.7(c). If we use the matrix representation for the state vectors $|\tilde{\Phi}_i\rangle$ and $|\tilde{\Psi}_{i-1}\rangle$, we can rewrite the above equation by the matrix product

$$\tilde{\Phi}_i = \left(\tilde{E}_i^{\text{L}} \right) \tilde{\Psi}_{i-1} \left(\tilde{E}_i^{\text{R}} \right)^\dagger \quad (3.15)$$

among $\tilde{E}_i^{\text{L}}(s_i' \zeta_{i-1}' | s_i \zeta_{i-1})$, $\tilde{\Psi}_{i-1}(s_i \zeta_{i-1} | \sigma_i \xi_{i-1})$, and the transpose of $\tilde{E}_i^{\text{R}}(\sigma_i' \xi_{i-1}' | \sigma_i \xi_{i-1})$. The structure of $\tilde{E}_i =$

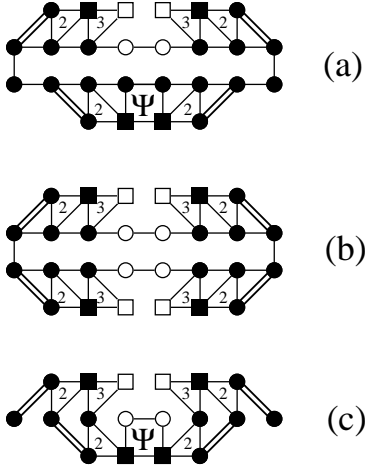


Fig. 7. Graphical representations: (a) $\tilde{P}_i |\tilde{\Psi}_{i-1}\rangle$ in Eq.(2.19)' in case of $i = 4$. (b) $\tilde{T}_i \equiv \tilde{T}_i^L \cdot W \cdot \tilde{T}_i^R$. (c) $\tilde{E}_i |\tilde{\Psi}_{i-1}\rangle$ in Eq.(3.14). The long rectangular in (a) and (b) represents \tilde{T}_i in Eq.(2.3). The triangle with number j represents the block spin transformation \hat{U}_j or \hat{U}_j^\dagger . The rectangular area labeled by “ Ψ ” represents $|\tilde{\Psi}_{i-1}\rangle$. Small circles and squares are original spins and block spins, respectively, where black ones are summed out. Two circles that are connected by the double lines represent the same spin. We have used Eq.(3.4), and therefore \hat{V}_1 is not explicitly drawn in the picture. Stacking (b) and (c) we obtain (a) when Eq.(3.7) is satisfied.

$\tilde{E}_i^L \cdot \tilde{E}_i^R$ is understood from Fig.7(c) without difficulty. As we explain in the following, $|\tilde{\Phi}_i\rangle$ is easily created from $|\tilde{\Psi}_{i-1}\rangle$.

It is not required to possess \tilde{E}_i^L and \tilde{E}_i^R explicitly for the construction of $\tilde{\Phi}_i$ in Eq.(3.15). Let us substitute the singular value decomposition of $\tilde{\Psi}_{i-1}$ to the r.h.s of Eq.(3.15). From the assumed symmetry of $\tilde{\Psi}_{i-1}$, the decomposition is equivalent to the diagonalization of $\tilde{\Psi}_{i-1}$ as

$$\tilde{\Psi}_{i-1} = \hat{U}_{i-1} \Omega_{i-1} \hat{U}_{i-1}^\dagger, \quad (3.16)$$

where Ω_{i-1} is a diagonal matrix, and the square of Ω_{i-1} represents the eigenvalues of the density matrix $\hat{\rho}_{i-1}^R = \tilde{\Psi}_{i-1}^\dagger \tilde{\Psi}_{i-1} = \hat{U}_{i-1} (\Omega_{i-1})^2 \hat{U}_{i-1}^\dagger$. Substituting Eq.(3.16) to $\tilde{\Psi}_{i-1}$ in Eq.(3.15), we obtain

$$\begin{aligned} \tilde{\Phi}_i &= \left(\tilde{E}_i^L \right) \hat{U}_{i-1} \Omega_{i-1} \hat{U}_{i-1}^\dagger \left(\tilde{E}_i^R \right)^\dagger \\ &= \left(\tilde{E}_i^L \hat{U}_{i-1} \right) \Omega_{i-1} \left(\tilde{E}_i^R \hat{U}_{i-1}^\dagger \right)^\dagger \\ &= \tilde{A}_i \Omega_{i-1} \tilde{A}_i^\dagger, \end{aligned} \quad (3.17)$$

where $\tilde{A}_i \equiv \tilde{E}_i^R \hat{U}_{i-1}$ and we have used the assumed symmetry $\tilde{E}_i^L = \tilde{E}_i^R$. From the recursion relation of \tilde{E}_i^R in Eq.(3.10) the new matrix \tilde{A}_i satisfies the recursion relation

$$\begin{aligned} \tilde{A}_i &= \tilde{E}_i^R \hat{U}_{i-1} = \left[\hat{U}_{i-1}^\dagger \left(id \cdot \tilde{E}_{i-1}^R \right) \hat{U}_{i-2} \right] \hat{U}_{i-1} \\ &= \left[\hat{U}_{i-1}^\dagger \left(id \cdot \tilde{E}_{i-1}^R \hat{U}_{i-2} \right) \right] \hat{U}_{i-1} \end{aligned}$$

$$= \left[\hat{U}_{i-1}^\dagger \left(id \cdot \tilde{A}_{i-1} \right) \right] \hat{U}_{i-1}. \quad (3.18)$$

The initial condition of this relation is obtained from the definition of \tilde{E}_i^R in Eq.(3.9). Substituting $\tilde{E}_3^R = \hat{U}_2^\dagger I_3 \hat{V}_1$ to $\tilde{A}_3 = \tilde{E}_3^R \hat{U}_2$ we obtain $\tilde{A}_3 = (\hat{U}_2^\dagger I_3 \hat{V}_1) \hat{U}_2 = \left[\hat{U}_2^\dagger (id \cdot \hat{V}_1) \right] \hat{U}_2$, and thus we find the initial condition

$$\tilde{A}_2 = V_1. \quad (3.19)$$

It might be helpful to rewrite Eq.(3.18) by the element:

$$\begin{aligned} \tilde{A}_i(\sigma_i \xi_{i-1} | \eta_i) &= \sum_{\sigma_{i-1} \xi_{i-2} \eta_{i-1}} U_{i-1}(\sigma_{i-1} \xi_{i-2} | \xi_{i-1}) \\ &\times \tilde{A}_{i-1}(\sigma_{i-1} \xi_{i-2} | \eta_{i-1}) U_{i-1}(\sigma_i \eta_{i-1} | \eta_i). \end{aligned} \quad (3.20)$$

Figure 8 shows the graphical representation of Eqs.(3.18) and (3.20).

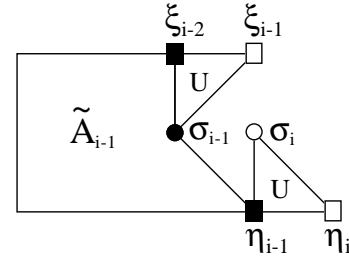


Fig. 8. Recursive relations of \tilde{A}_i . $\tilde{A}_i = \left[\hat{U}_{i-1}^\dagger \left(id \cdot \tilde{A}_{i-1} \right) \right] \hat{U}_{i-1}$ for $i \geq 4$ in Eqs.(3.18) and (3.20).

Using the recursion relation Eq.(3.18) and the approximation from Eq.(2.19)' to Eq.(3.13), let us reformulate the recursive creation of the state vectors proposed in the previous section. Suppose that we have the renormalized transfer matrix \tilde{T}_{i-1} , the state vector $|\tilde{\Psi}_{i-1}\rangle$ and the matrix \tilde{A}_{i-1} . We obtain $|\tilde{\Psi}_i\rangle$ as follows.

- Perform the diagonalization $\tilde{\Psi}_{i-1} \rightarrow \hat{U}_{i-1} \Omega_{i-1} \hat{U}_{i-1}^\dagger$ in Eq.(3.16) to obtain U_{i-1} and Ω_{i-1} .
- Obtain $\tilde{A}_i = \left[\hat{U}_{i-1}^\dagger \left(id \cdot \tilde{A}_{i-1} \right) \right] \hat{U}_{i-1}$ by Eq.(3.18).
- Extend the linear dimension of the renormalized transfer matrix by $\tilde{T}_i^R = \hat{U}_{i-1}^\dagger \left(W \cdot \tilde{T}_{i-1}^R \right) \hat{U}_{i-1}$ in Eq.(3.3) and the same for \tilde{T}_i^L .
- Obtain $\tilde{\Phi}_i = \tilde{A}_i \Omega_{i-1} \tilde{A}_i^\dagger$. (Eq.(3.17).)
- Multiply \tilde{T}_i to $|\tilde{\Phi}_i\rangle$. Admitting the approximation from Eq.(2.19)' to Eq.(3.13), substitute the obtained vector $\tilde{T}_i |\tilde{\Phi}_i\rangle$ to $|\tilde{\Psi}_i\rangle$ and proceed to the next iteration.

With use of this recursive calculation, we obtain the state vectors and the partition functions explained in the previous section. (The obtained data is of use for the finite size scaling at the criticality.²⁵⁾)

The recursive calculation starts from the initial condition given by Eq.(3.19). The calculation can be stopped when the observed physical quantities, such as the free energy per site, converge to their values at the large

system size limit. Alternatively, the difference between $\hat{\rho}_i^R/\tilde{Z}_i$ and $\hat{\rho}_{i+1}^R/\tilde{Z}_{i+1}$ (or in some cases $\hat{\rho}_i^R/\tilde{Z}_i$ and $\hat{\rho}_{i+2}^R/\tilde{Z}_{i+2}$) can be used for the confirmation of the convergence, since when i is several times larger than the correlation length the recursive procedures (a)-(e) becomes just the repetition of the same calculation. It should be noted that even in the large i limit the condition $\hat{U}_{i+1} = \hat{U}_i$ is not always satisfied, as reported by Okunishi *et al.*²⁰⁾

The recursive process (a)-(e) is actually a special case of the numerical algorithm of the ‘product wave function renormalization group (PWFRG) method’.¹⁵⁾ In order to clarify this point let us consider the numerical problem of obtaining the largest-eigenvalue eigenvector of the renormalized transfer matrix \tilde{T}_i during the calculation by infinite system DMRG method. Normally one of the power, the Lanczos, the Davidson, or the Arnoldi methods is employed for the diagonalization of \tilde{T}_i . The computational time required for these diagonalization methods is greatly dependent on the choice of the initial vector, and therefore it is important to create a good initial (or trial) vector for the diagonalization of \tilde{T}_i . From the arguments in the previous section — see Eqs.(2.19) and (2.20) — it is apparent that $|\tilde{\Psi}_i\rangle = \tilde{P}_i |\tilde{\Psi}_{i-1}\rangle$ in Eq.(2.19)’ is a candidate of the initial vector. (The choice is not so bad if the correlation length of the system is much shorter than the system size $2i$, as was explained in the paragraph that contains Eq.(2.4), and expected to be of use for modest system size.) Since \tilde{P}_i is further approximated by $\tilde{T}_i \tilde{E}_i$, we can say that \tilde{E}_i has a function of extending the vector dimension of $|\tilde{\Psi}_{i-1}\rangle$ to create $|\tilde{\Phi}_i\rangle = \tilde{E}_i |\tilde{\Psi}_{i-1}\rangle$ in Eq.(3.14), and that \tilde{T}_i improves $|\tilde{\Phi}_i\rangle$ to give an approximation for $|\tilde{\Psi}_i\rangle$. We find that $|\tilde{\Phi}_i\rangle$ is also of use as the initial vector, since the diagonalization methods creates $\tilde{T}_i |\tilde{\Phi}_i\rangle \sim |\tilde{\Psi}_i\rangle$, $(\tilde{T}_i)^2 |\tilde{\Phi}_i\rangle \sim \tilde{T}_i |\tilde{\Psi}_i\rangle$, $(\tilde{T}_i)^3 |\tilde{\Phi}_i\rangle \sim (\tilde{T}_i)^2 |\tilde{\Psi}_i\rangle$, etc., inside their numerical procedure, and therefore to start the diagonalization from $|\tilde{\Phi}_i\rangle$ is almost as efficient as to start from $|\tilde{\Psi}_i\rangle$.

Based on the above discussion about the initial vector, we find that the recursion relation Eq.(3.18) can be efficiently used for the numerical acceleration of the infinite system DMRG algorithm. The way is simply to replace the step (e) of the recursive calculations (a)-(e) by

(e’) Using $|\tilde{\Phi}_i\rangle$ as the initial vector for the Lanczos diagonalization (or Davidson, Arnoldi diagonalization or the power method)²⁸⁾ of \tilde{T}_i . Substitute the obtained largest-eigenvalue eigenvector of \tilde{T}_i to $|\tilde{\Psi}_i\rangle$ and proceed to the next iteration.

The modified recursive method, which consists of (a), (b), (c), (d), and (e’), is the numerical algorithm of the original version of the PWFRG method.¹⁵⁾ So far the initial condition of this method — the matrix element of \tilde{A}_2 — was set empirically. What we have clarified here is that the initial condition \tilde{A}_2 is given by V_1 in Eq.(3.19), which represent the boundary condition of the system.²⁹⁾ One can easily verify that the calculation by (a)-(e’) gives the same result as the infinite system DMRG method, since the DMRG method consists of (a), (c), and the

diagonalization of \tilde{T}_i .

Even with the use of the initial vector $\tilde{\Phi}_i$ the diagonalization step (e’) occasionally consume large amount of computational time. We can improve the situation, considering the half-way between (e) and (e’). For example, if we employ the Lanczos diagonalization, (e) or (e’) can be replaced by

(e’’) Using $|\tilde{\Phi}_i\rangle$ as the initial vector for the Lanczos diagonalization of \tilde{T}_i , perform only one or only a few Lanczos steps. Substitute the obtained Lanczos vector to $|\tilde{\Psi}_i\rangle$ and proceed to the next iteration.

This is a realistic choice if one already has a computational program of the infinite system DMRG method, and if only the physical quantities at the large system size limit $i \rightarrow \infty$ is required.¹⁸⁾

If we store all the block spin transformations $\hat{U}_2, \hat{U}_3, \dots, \hat{U}_{i-1}$ obtained successively at the step(a), we implicitly have the variational MPS⁶⁻¹⁰⁾

$$\left[\hat{U}_2 \cdots \hat{U}_{i-1} \right] \Omega_{i-1} \left[\hat{U}_{i-1}^\dagger \cdots \hat{U}_2^\dagger \right], \quad (3.21)$$

which approximates $|\Psi_{i-1}\rangle$. The formulation can be obtained by considering the structure of $\langle \tilde{\Psi}_{i-1} | \tilde{T}_{i-1} | \tilde{\Psi}_{i-1} \rangle$ which well approximates $\langle \Psi_{i-1} | T_{i-1} | \Psi_{i-1} \rangle$. The fact enables us to use the iterative process of the PWFRG method (a)-(e’), combine with the finite system DMRG method. For example, the process (a)-(e’) can be used for the initial set-up of the variational MPS, that are further improved by the finite system DMRG sweeps. Equally, after finishing the finite system DMRG calculation for a certain system size $2N$, one can switch to the process (a)-(e’) again, and after M iterations to obtain a good variational MPS for the next finite system DMRG sweep at the size $2(N + M)$. The step (e’) can be replaced by (e) or (e’), since the finite system DMRG sweep improves the extended MPS. Such a switching process is of use when precise numerical data calculated by the finite system DMRG method are required for finite size scaling analyses.

§4. Conclusions and Discussions

We have explained the physical background of the PWFRG method from the view point of the MPS formalism. In section II, we first consider the calculation of the partition function of the IRF model on a finite size cluster. We observe the fact that the largest-eigenvalue eigenvector of a transfer matrix of width $2N$ can be approximated by the state vector that corresponds to lower half (in Fig.2(a)) of the system of width $2N$. By use of the fact, we construct an iterative numerical method to calculate the partition function up to arbitrary system size, which is equally of use as the CTMRG method.^{24, 25)} In Section III, we analyze the the whole structure of the renormalized transfer matrices, which appears in the formalism shown in §2. Observing the matrix product construction of the state vector, we find the way of increasing the number of matrices contained in MPS when we increment the system size. The extended MPS can be efficiently used as the initial vector for the diagonaliza-

tion of the renormalized transfer matrix, which appears in the infinite system DMRG method. As a result, we obtain the numerical algorithm of the PWFRG method. The initial condition for the PWFRG method, which has been set empirically, is clearly determined by Eq.(3.19) that corresponds to the boundary condition of the system.

The numerical method shown in §2 has clear physical meaning as the partition function calculation of finite size cluster of square shape. The same result can be obtained by the PWFRG method with the step (e) in the previous section. The PWFRG method with (e') gives exactly the same result as the infinite system DMRG method, where the calculation of the largest-eigenvalue eigenvector of the renormalized transfer matrix is faster than the conventional infinite system DMRG method. One can use the PWFRG method with (e'') if the convergence of the calculated physical quantities toward the large system size limit is slow with the use of (e) or (e'). The use of (e'') accelerates the convergence of the free energy per site, but the calculated data before completing the convergence do not have clear physical meaning. After the convergence, the PWFRG method with (e), (e') and (e'') give the same result about the thermodynamic limit of the system.

We comment that the PWFRG method can also be applied to 1D quantum systems, in addition to 2D classical systems.¹⁸⁻²² The simplest example is a uniform spin chain, whose Hamiltonian is written as a sum of position independent local terms h . In this case we obtain the superblock Hamiltonian $\tilde{H}_i \equiv \tilde{H}_i^L + h + \tilde{H}_i^R$ using the recursive relation $\tilde{H}_{i+1}^R \equiv \hat{U}_i^\dagger (h + \tilde{H}_i^R) \hat{U}_i$ similar to the extension process of the renormalized transfer matrix $\tilde{T}_{i+1}^R \equiv \hat{U}_i^\dagger (W \cdot \tilde{T}_i^R) \hat{U}_i$. Implementing the diagonalization of \tilde{H}_i into the recursive procedure in the PWFRG method (a)-(e') in §3, one can obtain the ground state property of the quantum system in the thermodynamic limit. As for the classical systems, use of (a)-(e'') is efficient for the acceleration of the convergence toward the large system size limit.

About the recursive creation of variational state for infinite 1D quantum Hamiltonians, the CTMRG method can also be employed for this purpose. Consider the infinite size chess board system generated by the Trotter decomposition^{30,31} applied to the density matrix $\exp(-\beta H)$ at zero temperature. If we divide the 2D lattice into 4 CTMs by cuts to the diagonal directions, the CTM at the top and the bottom corresponds to the variational state, and those at the left and the right correspond to the exponential of the corner Hamiltonian. This approach is quite similar to the system extension method explained in §2. In the limit of the zero imaginary time step in the Trotter decomposition, one obtains a DMRG formalism for the corner Hamiltonian. The formulation is similar to the recently proposed renormalization formalism on the corner Hamiltonian by Okunishi,³² but the block spin transformation is obtained from the diagonalization of the density matrix, instead of the diagonalization of the corner Hamiltonian.

A.G. is supported by the VEGA grant No. 2/3118/23.

- 1) S. R. White: Phys. Rev. Lett. **69** (1992) 2863; Phys. Rev. B **48** (1993) 10345.
- 2) *Density-Matrix Renormalization - A new numerical method in physics -*, eds. I. Peschel, X. Wang, M. Kaulke and K. Hallberg, (Springer Berlin, 1999), and references there in.
- 3) U. Schollwöck: Rev. Mod. Phys. **77** (2005) 259.
- 4) T. Nishino: J. Phys. Soc. Jpn. **64** (1995) 3598.
- 5) M. Fannes, B. Nachtergale and R. F. Werner: Europhys. Lett. **10** (1989) 633; Commun. Math. Phys. **144** (1992) 443; Commun. Math. Phys. **174** (1995) 477.
- 6) S. Östlund and S. Rommer: Phys. Rev. Lett. **75** (1995) 3537.
- 7) S. Rommer and S. Östlund: Phys. Rev. B **55** (1997) 2164.
- 8) M. Andersson, M. Boman, and S. Östlund: Phys. Rev. B **59** (1999) 10493.
- 9) H. Takasaki, T. Hikihara, and T. Nishino: J. Phys. Soc. Jpn. **68** (1999) 1537.
- 10) F. Verstraete, J.J. García-Ripoll, and J.I. Cirac: Phys. Rev. Lett. **93** (2004) 207204.
- 11) F. Verstraete, D. Porras, and J.I. Cirac: Phys. Rev. Lett. **93** (2004) 227205.
- 12) V. Murg, F. Verstraete, and J.I. Cirac: cond-mat/0501493.
- 13) S.R. White and I. Affleck: Phys. Rev. B **54** (1996) 9862.
- 14) S.R. White: Phys Rev Lett. **77** (1996) 3633.
- 15) T. Nishino and K. Okunishi: J. Phys. Soc. Jpn. **64** (1995) 4084.
- 16) N. Akutsu and Y. Akutsu: Phys. Rev. B **57** (1998) R4233; N. Akutsu and Y. Akutsu: Prog. Theor. Phys. **105** (2001) 123.
- 17) N. Akutsu, Y. Akutsu, and T. Yamamoto: Prog. Theor. Phys. **105** (2001) 361; N. Akutsu, Y. Akutsu, and T. Yamamoto: Phys. Rev. B **64** (2001) 085415; N. Akutsu, Y. Akutsu, and T. Yamamoto: Journal of Crystal Growth **237-239** (2002) 14; N. Akutsu, Y. Akutsu, and T. Yamamoto: Phys. Rev. B **67** (2003) 125407.
- 18) Y. Hieida, K. Okunishi and Y. Akutsu: Phys. Lett. A **233** (1997) 464.
- 19) M. Hagiwara, Y. Narumi, K. Kindo, M. Kohno, H. Nakano, R. Sato, and M. Takahashi: Phys. Rev. Lett. **80** (1998) 1312.
- 20) K. Okunishi, Y. Hieida, and Y. Akutsu: Phys. Rev. B **59** (1999) 6806; K. Okunishi, Y. Hieida, and Y. Akutsu Phys. Rev. E **59** (1999) R6227; Y. Hieida, K. Okunishi, and Y. Akutsu: New Journal of Physics **1** (1999) 7.1; K. Okunishi, Y. Hieida, and Y. Akutsu: Phys. Rev. B **60** (1999) R6953; Y. Hieida, K. Okunishi, and Y. Akutsu: Phys. Rev. B **64** (2001) 224422.
- 21) Y. Narumi, K. Kindo, M. Hagiwara, H. Nakano, A. Kawaguchi K. Okunishi, and M. Kohno: Phys. Rev. B **69** (2004) 174405.
- 22) S. Yoshikawa, K. Okunishi, M. Senda and S. Miyashita: J. Phys. Soc. Jpn. **73** (2004) 1798.
- 23) R.J. Baxter: *Exactly Solved Models in Statistical Mechanics* (Academic Press, London, 1982).
- 24) T. Nishino and K. Okunishi: J. Phys. Soc. Jpn. **65** (1996) 891; J. Phys. Soc. Jpn. **66** (1997) 3040.
- 25) T. Nishino, K. Okunishi, and M. Kikuchi: Phys. Lett. A **213** (1996) 69.
- 26) The first condition can be easily removed, just by treating the left half of the system independently from the right half. To remove the second condition, one has to diagonalize the asymmetric density matrix to obtain bi-orthogonal block spin transformations.
- 27) The shape of the cluster in Fig.1 is close to that was treated by Baxter in his method of CTM.²³
- 28) The Lanczos, the Davidson, and the Arnoldi diagonalizations can be interpreted as improvements of the power method.
- 29) We list the correspondence of the procedures (a)-(e') to equations in Ref.[15]: (a) \rightarrow Eq.(5),¹⁵ (b) \rightarrow Eq.(7),¹⁵ (c) \rightarrow Eq.(6),¹⁵ (d) \rightarrow Eq.(3),¹⁵ (e') \rightarrow Eq.(4).¹⁵
- 30) H. F. Trotter: Proc. Am. Math. Soc. **10** (1959) 545.
- 31) M. Suzuki: Prog. Theor. Phys. **56** (1976) 1454.
- 32) K. Okunishi: preprint, cond-mat/0507195.